Energy Impact of Ventilation and Air Infiltration
14th AIVC Conference, Copenhagen, Denmark
21-23 September 1993

Multizone Cooling Model for Calculating the Potential of Night Time Ventilation

J van der Maas, C-A Roulet

Laboratoire d'Energie Solaire et de Physique du Bâtiment, Ecole Polytechnique Fédérale de Lausanne, CH-1015 Lausanne, Switzerland

SYNOPSIS

One of the options to increase the energy efficiency of buildings in the cooling season, is to extract heat from the building envelope during the night by natural or forced ventilation. The exploitation of this technique by architects and designers requires the development of guide lines and a predesign tool showing how the potential cooling power depends on the influence of opening sizes and positions and on the interaction with the thermal mass.

While a single zone model is sufficient to estimate rougly the heat extracted from the building, a multi zone extension allows one to predict the distribution of air and wall temperatures and therefore the distribution of cooling power over the air flow path (when the zones are ventilated in series).

A zonal cooling model based on the principles of mass and energy conservation and coupling ventilation with both heat transfer and a thermal model for the walls.

The parameters of the ventilation model are the size and position of the openings, the stack height, and climatic parameters like temperature swing and wind characteristics. The heat transfer is parametrized by the exposed surface area of thermal mass, while the heat storage for heavy weight constructions is only characterized by both that surface area and the thermal effusivity of the exposed wall material.

The predictions are compared with measurements for a simple flow path configuration.

LIST OF SYMBOLS

ACH	Air changes per hour (1/h)
A_i	area of opening i (m^2)
α	Thermal diffusivity, $\alpha=\lambda/\rho c$ (m^2/s)
$b_{eff}(m)$	Effective wall thermal effusivity of zone m (J/ (m^2 K.$s^{0.5}$))
Bi	Biot number hL/λ (-)
b	Thermal effusivity, $b=\sqrt{(\lambda\rho c)}$ [J/ (m^2 K.$s^{0.5}$)]
C_d	Discharge coefficient
C_p	Thermal heat capacity of air (J/kgK)
C_{pi}	wind pressure coefficient at opening i
$C_s(m)$	Fraction of S(m) for convective heat transfer
c	Thermal heat capacity (J/kgK)
δ	Diffusion length, $\delta=\sqrt{(\alpha t)}$ (m)
d	Wall thickness (m)
$\Phi_g(m)$	Auxiliary heat gain in zone m (W)
Fo	Fourier number, $\alpha t/L^2$ (-)
Φ	Heat flow rate (W)
$\Phi_v(m)$	Ventilative heat gain in zone m (W)

$\Phi_w(m)$	Wall surface heat gain in zone m (W)
g	Acceleration of gravity (m/s^2)
$g_c(m)$	Convective fraction of auxiliary heat gain in zone m (W)
H	Height between centers of inlet and outlet opening (m)
h	Global heat transfer coefficient (W/m^2K)
z(m)	Height above reference of bottom of zone m (m)
h(m)	Height above reference of air node in zone m (m)
h_c	Convective heat transfer coefficient (W/m^2K)
zb(m)	Bottom opening between zones m and m+1 (m)
zt(m)	Top opening between zones m and m+1 (m)
i	Opening index : 1, 2
L	Characteristic length (m)
λ	Thermal conductivity (W/mK)
$\dot{m}$	Mass flow rate (kg/s)
m	Zone index : 1..N
p	Pressure (Pa)
p_s	Stack pressure (Pa)
p_w	Wind pressure (Pa)
Q	Volume flow rate (m^3/s)
ρa	Height weighted mean inside air density (kg/m^3)
$\rho(m)$	Air density in zone m (kg/m^3)
ρ_0	Air density at 273 K, 1.29 (kg/m^3)
ρ_{ext}	External air density (kg/m^3)
ρ	Density (kg/m^3)
r	Gas constant for air, 287 (J/kgK)
S(m)	Total internal wall surface area of zone m (m^2)
$S_k(m)$	Surface area of internal wall k in zone m (m^2)
T_0	Absolute temperature at 0°C, 273 K.
T	average absolute air temperature (K)
$T_a(m)$	Characteristic air temperature in zone m (K)
T_{ext}	external air temperature (K)
T_{in}	inside air temperature (K)
$T_w(m)$	Characteristic wall temperature in zone m (K)
T	inside outside air temperature difference (K)
t	time (s)
$u_{i<}$	Air velocity, outflow, in opening i (m/s)
$u_{i>}$	air velocity, inflow, in opening i (m/s)
u_w	wind reference velocity (m/s)
V	Volume (m^3)
W_i	Width of opening i (m)

1. INTRODUCTION

One of the options to increase the energy efficiency of buildings in the cooling season, is to extract heat from the building envelope during the night by natural or forced ventilation. The exploitation of this technique by architects and designers requires the development of guide lines and a predesign tool showing how the potential cooling power depends on the influence of opening sizes and positions and on the interaction with the thermal mass. Before discussing in more detail this option, it is instructive to briefly review situations where the ventilation strategy for cooling differs.

Three types of ventilative cooling situations can be distinguished giving more or less importance to the link between ventilation and the thermal mass of the building.

(i) Cooling the human body by ventilation. First the situation where the outside air temperature is close to the building temperature so that the structure can not be cooled by ventilation alone (no link between ventilation and thermal mass).

However wind induced ventilation through open windows can cool the human body and increase comfort. The heat transfer coefficient between the skin and the air increases with higher air speed, and also when the air is not very humid, the evaporation is enhanced and the body is cooled. This type of ventilative cooling plays a basic role in increasing comfort in warm climates.

The cooling effect of ceiling fans in summer falls also in this category.

(ii) Cooling with high air temperatures. When the air temperature is higher than the building structure, one strategy is to reduce ventilation so that the occupant experiences the coolth of the inside building surfaces. Another strategy is to maximize the cooling of the ventilation air by the building mass and to provide in addition increased comfort through ventilative cooling of the human body. To keep the inside of the building cool the designer should reduce solar heat gains as much as possible by installing shading devices.

A particular situation arises when high inside air temperatures result from internal heat gains. This situation is characterized by air temperatures which are much higher than the wall temperatures. To reduce the capacity of cooling equipment the designer needs to know how the inside temperature depends on the ventilation rate and on the thermal mass.

(iii) Cooling the building structure. At night, the outside air is often lower in temperature than the building structure, so that the latter can be cooled by ventilation. But how to optimize the cooling? The sometimes heard statement, that "the building structure can be potentially cooled to the outside air temperature" is self-contradictory. This is because when the building is at the air temperature no heat transfer can occur. Indeed, during the cooling process the inside air temperature is always somewhere half-way between the outside air temperature and the wall surface temperature.

To optimize ventilative cooling the designer should understand the link between ventilation, heat transfer and the distribution of thermal mass. While a large number of detailed building simulation models are available for the designer (see Ref. [1] and documents of IEA/ECB Annex 21), few experimental data on the cooling effect of ventilation are available in the literature.

In this paper we concentrate on the development of a simplified calculation method providing the needed output (energy, temperatures) using predesign input parameters (overall dimensions, average thermal properties of the building). The

model will be tested and improved by comparing with experimental data obtained on increasingly complex real configurations.

In the following we present new results on a simple configuration, the effect of natural ventilation at night on the cooling of the central stairwell of a three storey building. The data are interpreted with a zonal cooling model based on the principles of mass and energy conservation.The air temperature of each zone follows from an energy balance between the ventilative cooling rate, the heat gain and the heat transfer to the wall.

A multi zone extension of the single zone model [Ref 2] gives additional information on the distribution of heat loss-rates and temperatures over the air flow path. (the zones are ventilated in series). Measurements for a single flow path configuration are analysed with an eight zone model. The thermal response of the stairwell is determined from an independent experiment as in [Ref 2]. The limits of the model are discussed and briefly compared with detailed simulation models like COMIS and ESP.

2. VENTILATION MODELING

The cooling rate induced by ventilation is proportional to the mass flow rate. For single and multiple flow paths through the building, these flow rates can be determined by setting up a resistance and pressure network. But the ventilation model will be chosen as simple as possible to include only the parameters which play an important role for limiting high flow rates.

Multi-zone air flow modeling is possible with multizone air flow simulation programmes like ESP and COMIS. These programmes have been mostly tested for small flow rates and validation of the COMIS programme is part of the work in the IEA/ECB Annex 23.

An important source of uncertainty in the output of air flow simulation programmes is due to the input parameters. The total flow resistance over the flow path is often not easy to formulate (doors, shafts, corridors, window) and this paper will be limited to a single air flow path.

2.1 Single zone

An example of a simplified air flow algorithm which contains the main features needed here is "AIDA" [3]. It calculates the inside pressure for which the flow balance equation in a single zone enclosure with small openings is satisfied. The flow through each opening is found from the difference between the inside pressure and the sum of the wind and stack pressures. The algorithm can easily be developed to include large openings (i.e. where two-way flow can occur) either by defining a large opening as a series of stacked horizontal slits, or by using the Cockroft algorithm which is implemented in ESP [4]. It is also possible to include temperature stratification by defining the inside temperature as a function of height.

Because the fluctuating wind pressure effect is not included in the model it is discussed briefly.

Fluctuating pressures. The AIDA algorithm can be used to illustrate the variation of the inside pressure and therefore of the position of the neutral pressure level when openings or wind pressures are changed. When the wind velocity or direction are changing and the inside pressure increases, it takes some time before a sufficient amount of air has entered the building for the inside pressure to built up a new

equilibrium value. This time increases with the zone volume. Fluctuating wind velocity and direction can therefore induce air flows that become important in absolute value when the zone volume behind the opening is large.

Fluctuating neutral level. Fluctuating internal pressures also cause the neutral level to vary with height. The case of a single zone enclosure with two openings (area A_t at the top and A_b at the bottom) at a vertical distance H, has an analytical solution which gives the same flowrates as the AIDA algorithm. The neutral level for this single zone case is situated at a distance h from the top opening where [5]

$$h = \frac{H}{\left[1 + (T_{out} / T_{in})(A_t / A_b)^2\right]} \qquad (1)$$

This relation depends on the mass flow balance and h is not dependent on the flow rate. The wind will mainly modify the internal pressure. On the other hand, a fluctuating wind requires continuous adjustment of the mass flow balance, causing a fluctuation of the neutral level. Such conditions reduce the precision with which the air change rate can be determined. In particular the velocity profile in a large opening may vary continuously and the use of tracer gas techniques becomes unreliable.

2.2 Multi zone ventilation model

A multi-zone single flow path configuration is defined when N zones or rooms are ventilated in series. The total driving force, the sum of stack and wind pressures can be calculated from the zone air temperatures and the pressure coefficients.

The single flow path is divided in N successive 'zones' ($N \geq 1$), which are conveniently chosen in order to have nearly constant physical properties (air density for example). This choice will be further discussed in connection with the thermal model. Only for N=1 the outlet and inlet are in the same zone, else both are in different zones.

The stack pressure is then calculated by integrating the air density $\rho(z)$ over height along the flow path between the inlet at $z=z_0$ and the outlet at $z=z_N$. Assuming for each zone a constant air temperature, $T_a(m)$, many parameters would be needed to calculate this in detail, for example for each zone one would need to input the height of the air node, the height of the zone, the height and size of the interconnecting opening. Because the total stack pressure is not sensitive for the details of the density variation, a mean (height weighted) inside air density is used :

$$\overline{\rho_a} = \frac{1}{H}\int_{z_0}^{z_N} \frac{\rho_0 T_0}{T_a}\,dz \cong \frac{\sum_{m=1}^{N} \frac{\rho_0 T_0}{T_a(m)}(z(m+1)-z(m))}{\sum_{m=1}^{N}(z(m+1)-z(m))} \qquad (2)$$

where z(m) is the height of the bottom of zone m, and where z(m+1) corresponds to the top of the last zone. This definition will take into account the effect that zones at the same height do not enhance the stack pressure.

The stack pressure is now calculated as :

$$p_s = -\,g\,H\,(\rho_{ext} - \overline{\rho_a}) \qquad (3)$$

and the total air flow driving pressure, p, is obtained by adding the average wind pressure using local pressure coefficients :

$$p = p_s + p_w = p_s + (C_{p1} - C_{p2}) \frac{1}{2} \rho_{ext} u_w^2 \quad (4)$$

The Bernoulli equation states that in a non-viscous flow field where the stream lines have all the same origin, the sum of static and dynamic pressure is a constant.

$$\Delta p + \frac{1}{2} \rho u^2 = \text{constant} \quad (5)$$

The mass flow rate through the opening is then given by

$$\begin{aligned} \dot{m} &= \rho Q = \rho C_d A u \\ &= \rho C_d A \sqrt{2 \Delta p / \rho} \end{aligned} \quad (6)$$

For a number of openings in series, the mass flow is a constant but there is a partial pressure drop over each opening. Because the velocities vary inversely with the opening area (continuity equation) the pressure drop over successive openings varies inversely with the square of the area.

$$\Delta p = \sum_{i=1}^{n} (\Delta p)_i = \sum_{i=1}^{n} \frac{\rho}{2} u_i^2 = \frac{\dot{m}^2}{2\rho} \sum_{i=1}^{n} \left(\frac{1}{C_d A} \right)_i^2 \quad (7)$$

When n openings are placed in series an effective opening area, A_{eff}, can be defined as :

$$\left(\frac{1}{A_{eff}} \right)^2 = \left(\frac{1}{Cd_1 A_1} \right)^2 + \left(\frac{1}{Cd_2 A_2} \right)^2 + \ldots\ldots + \left(\frac{1}{Cd_n A_n} \right)^2 \quad (8)$$

In the formulation leading to Equation 7, non viscous flow was assumed and the apparent static pressure loss is due to the generation of dynamic pressures. However the formulation is similar when flow elements cause viscous pressure drops resulting in discharge coefficients lower than the usual value for sharp orifices of 0.6.

For the two opening single zone configuration this results in the well known stackflow expression [2,5]

$$\dot{m} = \rho_a(N) A_t C_d \sqrt{\frac{2g H (\overline{T_a} - T_{ext})}{T_{in} \left[1 + (T_{ext} / T_a(N)) (A_t / A_b)^2 \right]}} \quad (9)$$

where different in and outflow temperatures and a single discharge coefficient C_d ($\approx$0.6) are assumed. Comparing Eq.9 with Eq.1, two way flow is expected to occur when the neutral pressure level would fall inside the opening, i.e. when h is smaller than about half the height of the top opening or when (H-h) is smaller than half the height of the bottom opening.

For single sided ventilation through a window of height H and width W, the mass flow is expressed as [6-8] :

(9b) $$\dot{m} = \frac{1}{3} \rho_{ext} H W C_d \sqrt{\frac{g H (\overline{T_a} - T_{ext})}{T_{ext}}}$$

For a single flow path it is not necessary to know the neutral pressure level explicitly. Due to the vertical flow resisitances the neutral level will depend on the flow rate. It is worth noting however that when multiple openings occur at the top and bottom of the configuration, grouping is sometimes possible using Eq.8, and then Eq.1 applies again for the neutral level.

2.3 Cooling by ventilation

When the zonal air temperatures, $T_a(m)$, are known the cooling rate for each zone is immediately available. The air temperature entering zone m is at the temperature of the previous zone Ta(m-1) and leaves the zone at Ta(m). The ventilation heat loss, $\Phi_v(m)$, for zone m is therefore:

(10) $$\Phi_v(m) = \dot{m} C_p [T_a(m) - T_a(m-1)]$$

where $\dot{m}$, the air mass flow along the flowpath, is calculated from the ventilation model. The total ventilation heat loss from the flow path is

(11) $$\Phi_v = \sum_{m=1}^{N} \Phi_v(m) = \dot{m} C_p [T_a(N) - T_a(0)]$$

The zonal cooling rate $\Phi_v(m)$ should then be used in the heat balance for each zone.

3. THERMAL MODELING

The heat balance in the air node for each of the N-zones is obtained from the sum of the ventilation heat loss, $\Phi_v(m)$, the heat transferred by convection between the wall and the air, $\Phi_w(m)$, and the convective heat gain in zone m, $\Phi_g(m)$:

(12) $$\Phi_v(m) + \Phi_w(m) + \Phi_g(m) = 0$$

The heat flow at the wall-air interface in zone m depends on the convective heat transfer coefficient, h_c, and the internal surface area of zone m, S(m) :

(13) $$\Phi_w(m) = h_c S(m) [T_w(m,t) - T_a(m)]$$

In general the convectively active heat exchanging surface area is smaller than the total internal wall surface area of zone m. This is illustrated in Figure 1. The fraction of S(m) for convective heat transfer is $C_s(m)$, so that Eq.13 is modified into

(14) $$\Phi_w(m) = h_c\, C_s(m)\, S(m)\, [T_w(m,t) - T_a(m)]$$

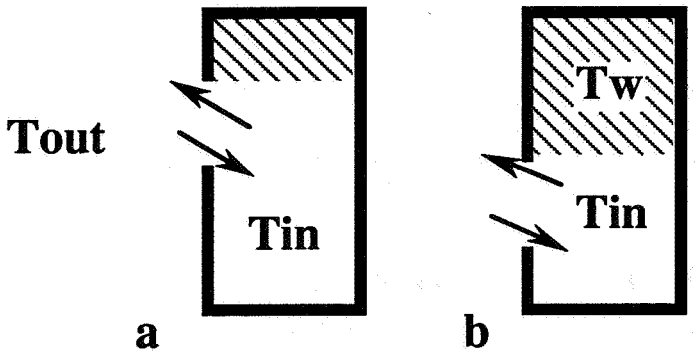

Figure 1. Above the upper level of the opening trapped warm air (dashed) is at the same temperature as the wall, the ceiling and wall surface above the top of the window do not cool by convection. The coefficient C_s is the fraction of the internal wall surface which is available for convective heat transfer and is about 0.8 in (a) and 0.4 in (b).

The wall surface temperature in zone m, $T_w(m,t)$, will respond to this heat flow and vary with time. A simple model for the surface temperature is used based on the solution of the heat equation for a semi-infinite wall.

3.1 Semi infinite wall model

There exists a convenient solution of the heat equation for a prescribed time variation of the heat flow rate at the surface if the wall is relatively thick and behaves for the duration of night cooling as a semi-infinite wall [2,6]. The application limits of this assumption will not be discussed here, but as an indication we note that the typical penetration depth of a 24 hr cycle heat wave in concrete is 10 to 15cm.

For a given heat flux density q(t)[W/m^2] the heat equation has an analytical solution for the case of a homogeneous semi-infinite wall, and the time dependence of the surface temperature of the wall, T_{wall}, is

(15) $$T_{wall}(t) - T_{wall}(0) = \frac{1}{b\sqrt{\pi}} \int_0^t q(t-\tau)\, \tau^{-1/2}\, d\tau$$

where $b=\sqrt{\rho c \lambda}$ (the square root of the product of thermal conductivity, density, and specific heat) is the thermal effusivity of the wall material.

For a single step in q, Equation 15 simplifies to

(16) $$T_{wall}(t) - T_{wall}(0) = \Delta T_{wall}(t) = \frac{2q}{b}\sqrt{\frac{t}{\pi}} = q\, R_{dyn}$$

and the increase in surface temperature is seen to vary as the square root of *elapsed time* since the step.

The superposition principle of the heat equation implies that when the function q(t) is given by a *sum of step functions* than the solution is given by a *sum of solutions* like Eq16 where time 't' is different for each step, being the elapsed time since the step happened.

In Reference [2] the heat flux during night cooling was a function of time, but instead of dealing with the exact time history of heat flux, a history of constant q was assumed at each time step. This is a useful approximation when q is close to the time averaged value. When this is not acceptable as a solution, the time history can be approximated to any desired accuracy by a sum of step functions.

3.2 Thermal zonal response

By applying a convective heat pulse to a closed zone m, the average heat flux at the wall will be $q = \Phi_w(m) / S(m)$ and it is observed that the air temperature increases (in accordance with Eqs 13 and 16) like

$$\Delta T_a(t)/q = \frac{2}{b}\sqrt{\frac{t}{\pi}} + 1/h_c\,(1-\exp(-t/\tau)) \qquad (17)$$

where the typical time constant for air and little furniture is usually 10-30 minutes.

After correction for background drift, $\Delta T_a(t)/q$ and $\Delta T_w(t)/q$, can be plotted as a function of $\sqrt{t}$, providing a constant rate of change with slope 1.13/b. This experimental parameter b is called the effective thermal effusivity b_{eff} and characterizes the thermal response of the zone [2,6].

The experimental parameter b_{eff} is related to the thermal properties of the individual walls k of the zone m. If the surface areas are $S_k(m)$, and the materials have nominal values for the thermal effusivities $b_k(m)$, there is the approximate relation :

$$b_{eff} \approx \frac{\sum_{k=1}^{n} S_k(m)\, b_k(m)}{\sum_{k=1}^{n} S_k(m)} \qquad (18)$$

where the sum over the n surfaces $S_k(m)$ should equal S(m). Instead of having all the 2n input parameters for the individual wall surfaces, it is more practical to estimate b_{eff}.

3.3 Multi zone cooling model

The ventilative cooling model is obtained when the thermal zone model and the ventilation model are coupled through the air node temperatures. In Figure 2 the multizone cooling model is given schematically for three zones. Details of the used algorithm are given in Annex 1.

With reference to Figure 2, the input parameters for each zone are :

- the exposed wall surface area S(m) and $C_s(m)$
- the effective thermal effusivity $b_{eff}(m)$
- the initial wall temperature $T_w(m)$
- the internal heat gain Φ_g (m)

The most elaborate input part would be the description of the time variation of the heat gain (this is to constitute input in the expression 15 and 16), and because this is not yet implemented, for the present tests Φ_g =0.

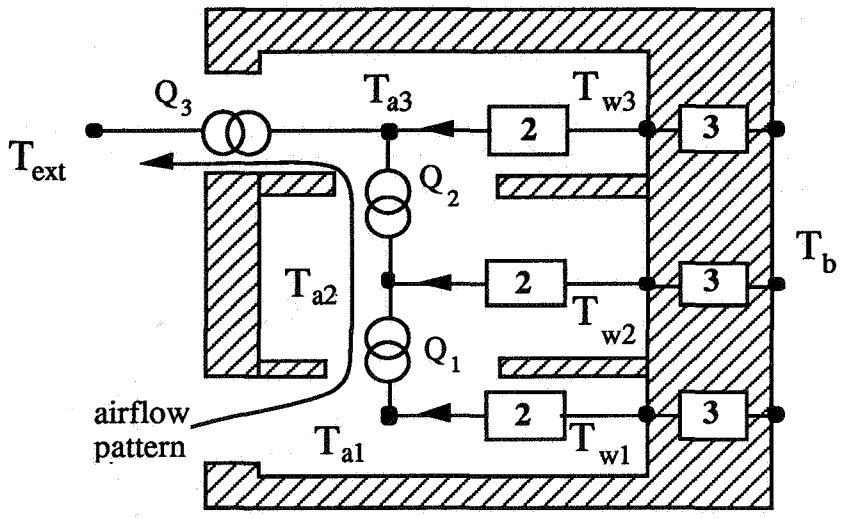

Figure 2. Multi zone cooling model with three zones. (2) are the heat transfer resistances and (3) is the dynamic wall resistance. The heat sources Q_i, represent the combined effect of internal heat gain and ventilation heat loss. For each zone the principles of mass and energy conservation apply assuming that in the dynamic regime the zones are only coupled through the air temperature nodes.

The (time dependent) output parameters for each zone are calculated from the external air temperature variation and are

- the air temperature $T_a(m,t)$
- the surface temperature $T_w(m,t)$
- the ventilative cooling load $\Phi_v(m,t)$

4. EXPERIMENTAL CONFIGURATION

4.1 LESO library

Some interesting preliminary observations have been made on the LESO library which is on the second (top) floor of the LESO building. The internal walls are of 10 cm concrete bricks and 8cm insulation. The external walls are thicker. On the west side there is a 1.5 meter wide, three meter high attic of one meter deep,which contains a 1.5 m high, 1m wide window. There is a light well in the ceiling. The volume of the room is 100 m^3, and the total internal wall surface area 120 m^2. The room is characterized by an average thermal effusivity of the walls of b=1000 [J/

(m^2 K.$s^{0.5}$)] with a 10% uncertainty, determined in a separate heater test with the window closed.

After opening a window, cold outside air enters and lowers the inside temperature and cools the wall surfaces. This configuration has been studied for various cases and the results were interpreted with a single zone model [6,7,8]. However it will be shown in the results section that the horizontal and vertical temperature stratification which had always been observed [7] can be understood with the multi zone model.

Air temperatures were measured with a hot wire anemometer. Wall temperatures were scanned with an infrared radiation thermometer which was frequently checked against thermo couple readings.

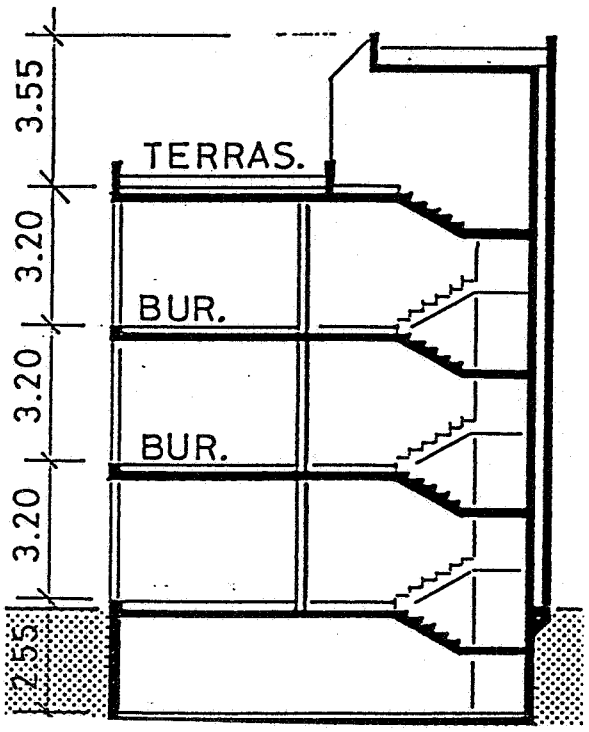

Figure 3. North-South cross-section of the central part of the LESO building. During the experiment the doors between the stairwell and the offices were closed.

4.2 LESO stairwell

The three level LESO-building, has occupied offices at levels 0, 1 and 2. The central stairwell extends from level -1 to the roof at level 3 and is about 12m high (Figure 3). The stairwell is ventilated at night by burglarproof openings at the entrance (1.04 m^2 effective ventilation area), and by the open roof door (1.78 m^2). The stairwell walls are made of light concrete bricks and the floors and flat roof of massive concrete. The offices are on the south side. All walls, floor, and ceiling have 10-20 cm glass wool insulation as a second layer. Experimental determination

of the thermal effusivity [2] yielded a value of b=1100 J/($m^2Ks^{0.5}$) with 10% uncertainty.

The total wall surface area of the stairwell (volume 4.5x8x15=540 m^3) is calculated to be 700 m^2 with a 10% uncertainty. The massive (20 to 30 cm thick) concrete stairwell itself is exposed on both sides and constitutes about 50% of the total heat-exchanging surface area.

Air and wall temperatures were measured with calibrated Pt100 temperature sensors and a datalogger system. The air temperature sensors were ventilated to avoid the influence of radiation by the warmer wall surfaces.

A heat flux probe was used with a stability and reproducibility better than 1W/m^2.

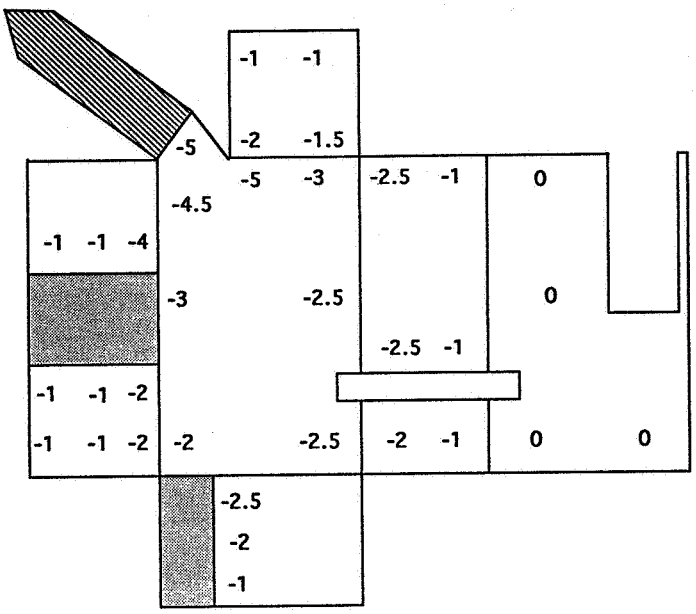

Figure 4. A layout of the library walls with a mapping of the drop in surface temperatures two hours after opening the window (T_{ext}=5°C). The floor is cooled strongly (north is to the right). The window is in the attic (grey) west.

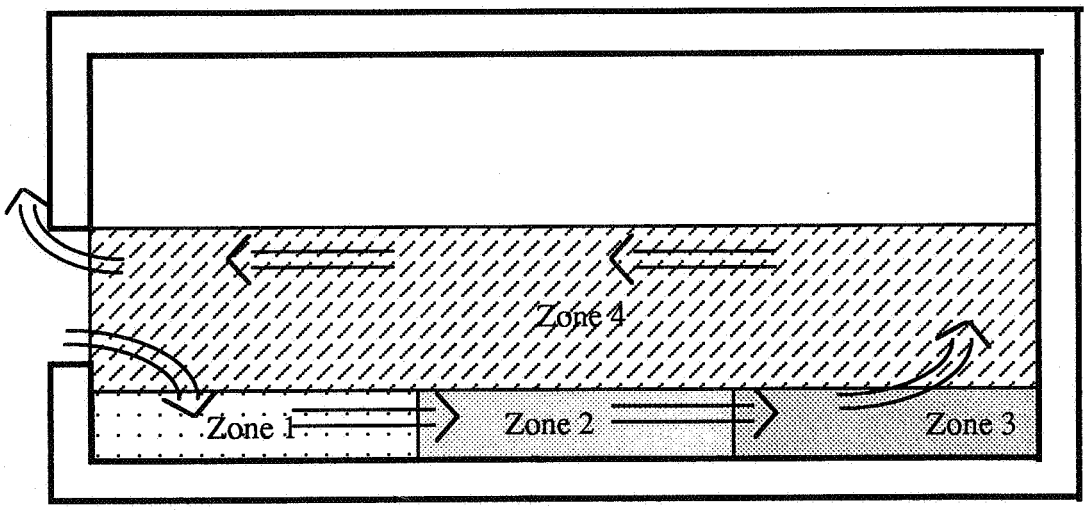

Figure 5. Air flow pattern and definition of zones for the multizone model

5. EXPERIMENTAL RESULTS

5.1 Results, LESO library

In Figure 4, is shown a map of the drop of inside wall surface temperatures after a period of two hours with the window open. Before opening the window, the space was in quasi thermal equilibrium with initial temperatures all over the walls (20±0.5)°C. The floor surface was cooled by as much as 3°C in front of the window. Above the top of the window level (compare Figure 1), the walls and ceiling temperature were not cooled by convection.

In Figure 5, is shown the dominating air circulation (a gravity current flows from the window to the backwall) and the division into four zones.

In Figure 6 the simulated surface and air temperatures are compared with measured data. Interestingly the horizontal and vertical temperature stratification is of the corect order of magnitude. For comparison, a single zone model would have taken the four zones together and predicting an air temperature of T_a=15.9 and a surface temperature T_w=18.8 over the whole zone.

This example demonstrates that the multizone model produces a more realistic temperature distribution. The dominating air flow pattern should be known in advance however. Because of the influence of radiation between the walls (which is not included in the model) the model tends to overpredict temperature stratification for long cooling times. It should not be difficult however to add to the model, a first order correction for radiative coupling between the ceiling and the floor.

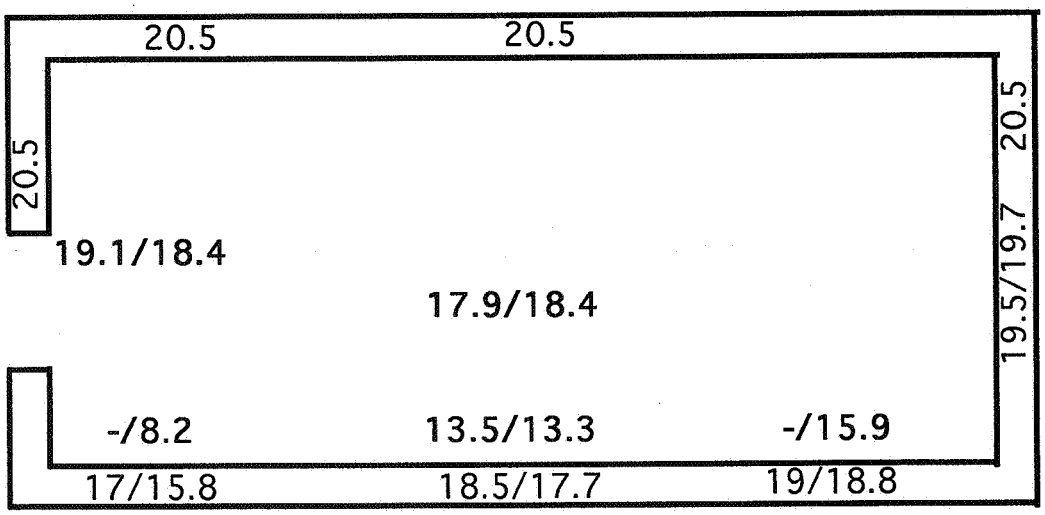

Figure 6. Cut through the library showing measured/simulated air (bold) and wall surface temperatures.

5.2 Results, LESO stairwell

In Figure 7 are shown the measured air temperatures between 7 and 17 april at three levels in the stairwell, the ground level, the second level and in the sunspace at rooflevel. In the evening of 12 april the top and bottom ventilation openings of the

stairwell were opened at 18.30 resulting in a ventilation rate of $1m^3/s$ (~7ACH) and the inside air temperatures decreased significantly. The external temperature during this night decreased linearly from 10 to 6°C.

In Figure 8 is given the vertical air temperature distribution in the center of the stairwell in the afternoon and at several moments during the night. In Figure 9, the wall-air temperature difference, which is significant for the heat transfer, is also plotted as a function of height.

It is worth noting that the large wall-air temperature difference resulted in clear boundary layer flow. The air velocity in the first centimeter of the wall was 0.3 to 0.4m/s while more than 0.1m from the surface this velocity was an order of magnitude smaller. This contrasts with the quite homogeneous velocity field encountered when the flow is driven by a fan or constant wind.

Figure 8 shows that the air temperature stratification is almost not changing during the cooling process. In Figure 9 the 3 to 4K temperature difference between the wall and the air corresponds to a heat flux of $15\text{-}20W/m^2$, a value which was confirmed by independent measurements with a heat flux meter. The total cooling power for this configuration was then of the order of 10kW for a temperature difference between the inside wall and outside air of about 10K.

To increase the cooling power, not only the opening area at ground level should be increased, but most important the wall surface area should be increased. In the LESO building this is most simply achieved by opening all the doors between the offices and the central stairwell.

To apply the multi-zone model the stairwell was divided in eight zones (Figure 10). The zones were chosen in order to assure that each temperature measuring point was respresentative for a zone (in its center). With this choice the multi zone model reproduces the features of Figures 8 and 9 (not shown).

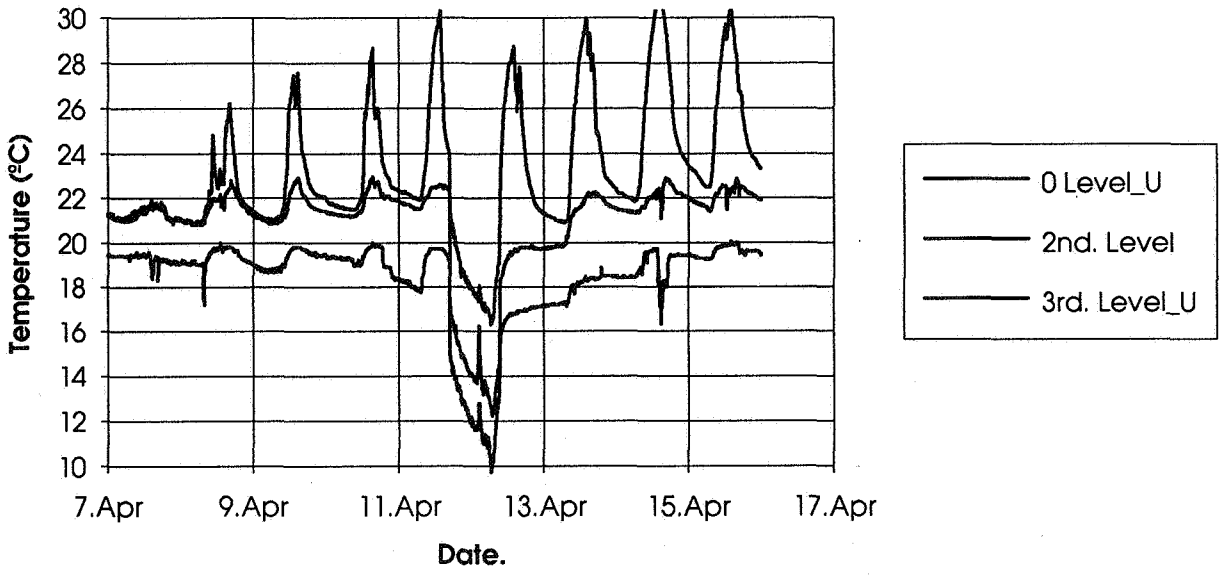

Figure 7. Observed air temperatures measured in the stairwell, at ground level, at the second level and in the sunspace (roof). In the night of 12 april the stairwell was ventilated and the air temperatures decreased significantly. The external temperature during this night decreased from 10 to 6°C.

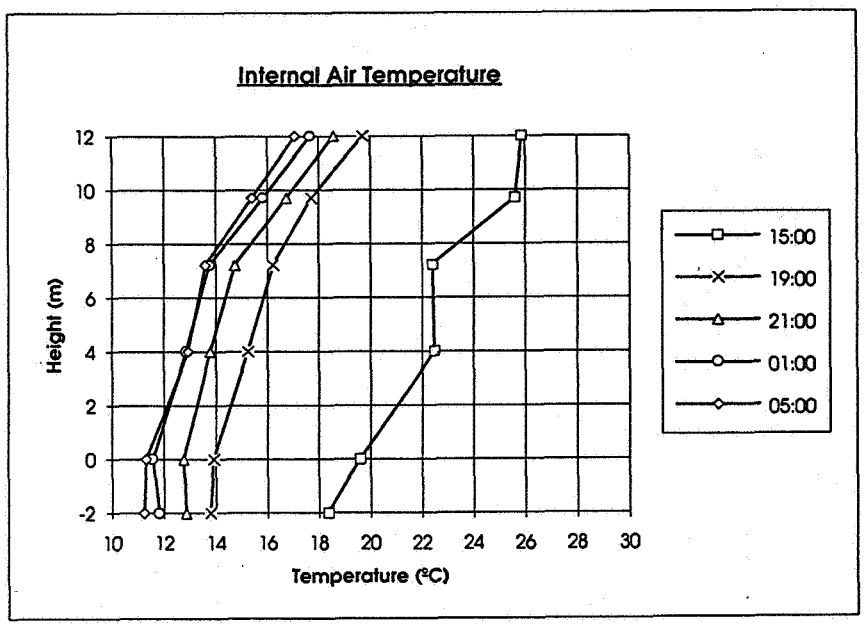

Figure 8. Observed air temperatures in the stairwell as a function of height above ground level.

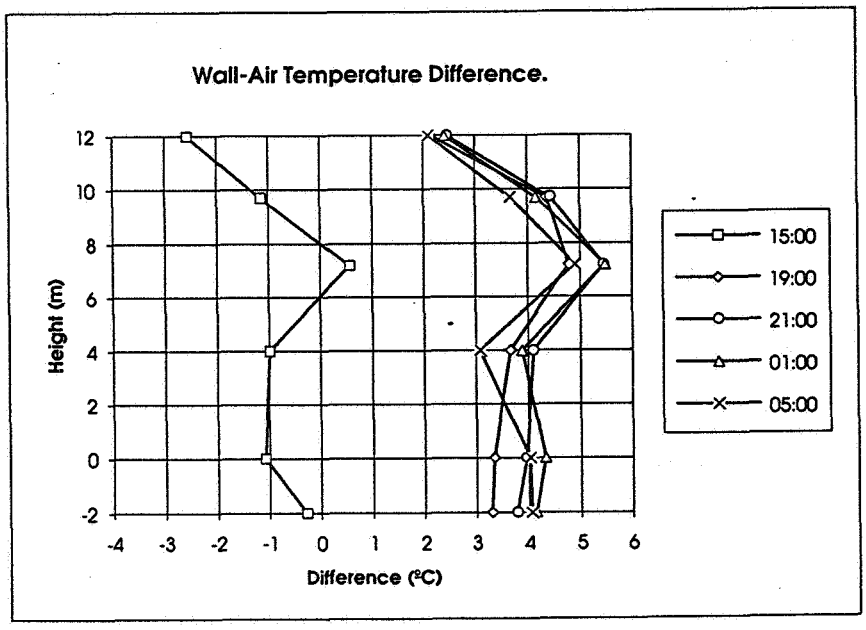

Figure 9. Observed wall-air temperature difference as a function of height above ground level.

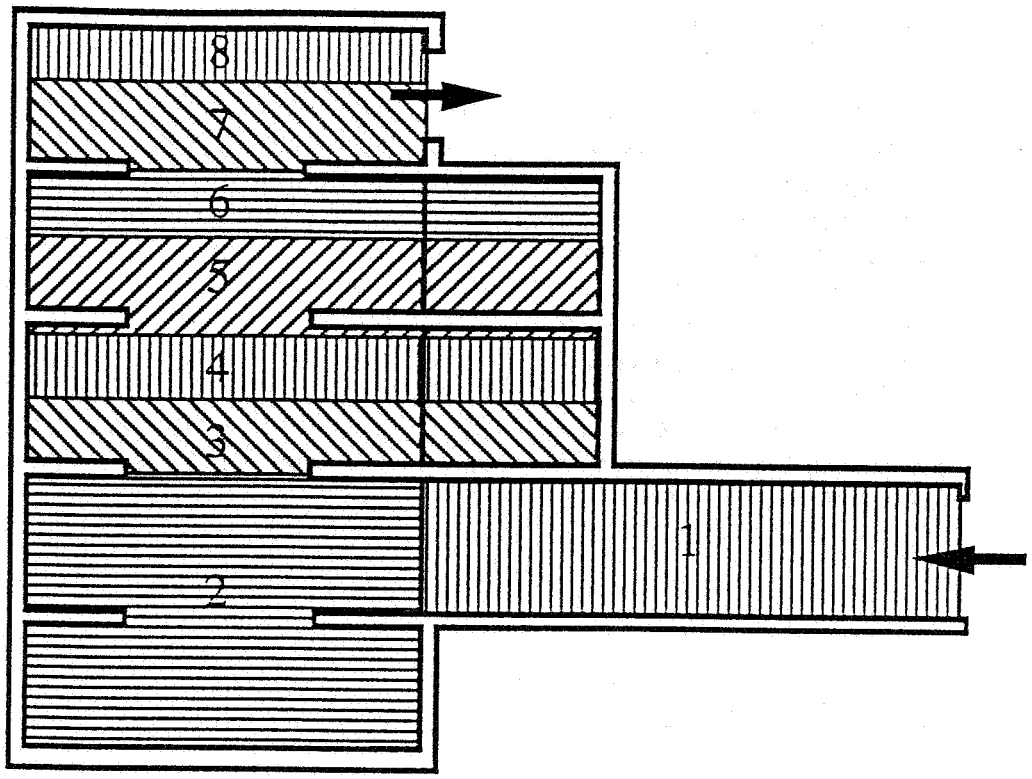

Figure 10. East-west stairwell section with indication of the eight zones used to compare with the experimentally measured temperatures.

6 DISCUSSION

The simplified model predicts correctly the order of magnitude of the temperature gradient for the case of single sided ventilation as shown in Figure 6. Further, the decrease in air and wall temperatures observed during night ventilation of a stairwell and shown in Figure 7 is also reproduced by the model (the details of the comparison between measurements and the model can not be shown in this paper).

A detailed comparison between the simplified model and more detailed building simulation models like ESP and COMIS will be performed. The first results show that for the particular problem under study (night ventilation over a single flow path) the simplified model explains the measured data sufficiently well requiring only few input parameters.

More detailed thermal modeling (e.g. with ESP) will be necessary in particular for the simulation of a building over longer time periods. Also the correct simulation of buildings that have low storage capacity and where the walls cannot be considered thick over a a one day period is reserved to detailed models .

While more detailed air flow modeling (e.g. COMIS) would be required when multiple flow paths occur, the latter imply an increased sensitivity of the output parameters for uncertainty in the input parameters.

More work must be done to learn how to define the limits of the zones. In particular when comparing with experiments, the calculated temperatures should be representative for the location of the temperature probes.

7 CONCLUSIONS

The effect of ventilative cooling was investigated and the data were analysed with a multi zonal cooling model based on the principles of mass and energy conservation.

Applied to the cooling by single sided ventilation, it is found that the multi zone model has the advantage over the single zone model [2] that it gives additional information on the distribution of heat loss-rates and temperatures over the air flow path. The model is limited to the case where the airflow pattern is known in advance and where it can be assumed that the zones are ventilated in series.

Measurements of the cooling of a stairwell by ventilation (single flow path configuration) are analysed with an eight zone model. The results show that the main features are reproduced. The model shows the influence of main design parameters like the opening position and size, and the exposed surface area of thermal mass, and its distribution.

8 ACKNOWLEDGEMENTS

The authors acknowledge research support from the Swiss Federal Office of Energy (OFEN, Switzerland). The assistance of Pierre-Yves Bridel and José-Antonio Rodriguez with the experiments and the data analysis was very much appreciated.

REFERENCES

[1] **Kendrick J., 1993.** "An overview of combined modelling of heat transport and air movement", Technical Note AIVC 40, Air Infiltration and Ventilation Centre, Coventry CV4 7EZ, GB.

[2] **van der Maas J. and C-A Roulet, 1991.** "Nighttime ventilation by stack effect". ASHRAE Transactions 1991,V.97,Pt. 1, 516-524.

[3] **Liddament M, 1989.** "AIDA - an air infiltration development algorithm", Air infiltration review, 11/1, p10-12; Palmiter L, 1990. "Mass flow for AIDA", AIR 11/2.

[4] **Clarke J A, 1985.** Energy simulation in building design, Adam Hilger Ltd, Bristol, UK; Cockroft J P 1979. "Heat transfer and air flow in buildings", PhD Thesis, Univ. of Glasgow.

[5] **ASHRAE. (1985).** 'ASHRAE handbook -1985 Fundamentals' Atlanta: American Society of Heating, Refrigerating, and Air-Conditioning Engineers, Inc.

[6] **Van der Maas J.(editor), Allard F., Haghighat F., Liébecq G., Pelletret R., Bienfait D., Vandaele L. and Walker R, 1992.** "Airflow through large openings in buildings", Technical Report of IEA/ECB-Annex 20: Air flow patterns within buildings. (EPFL/LESO-PB, CH-1015 Lausanne, Switzerland).

[7] **Van der Maas J, Roulet C -A, Hertig J -A, 1989.** "Some aspects of gravity driven airflow through large openings in buildings" ASHRAE Transactions 1989, Vol.95, Part 2, pp. 573-583

[8] **Van der Maas J., Roulet C.-A., 1990.** "Ventilation and Energy loss rates after opening a window", Air infiltration review, Vol 11, No 4,1990, pp 12–15

Annex 1

Multizone heat transfer algorithm for free cooling calculations

The algorithm is based on the repeated application of the single zone model along the flow path [2]. The path of constant massflow is divided into N zones : the mth zone is described by a heat exchanging surface area S(m), an initial wall surface temperature Tw0(m), and a wall parameter b(m). The only thermal coupling between the zones is through the ventilation network.

The air entering zone m is at the temperature of the previous zone Ta(m-1) and leaves the zone at Ta(m). The ventilation heat loss, $\Phi_v(m)$, for zone m is therefore:

(A1) $$\Phi_v(m) = \dot{m}\, C_p [T_a(m) - T_a(m\text{-}1)] = \dot{m}\, C_p\, \delta T(m)$$

where $\dot{m}$, the air mass flow along the flowpath, is calculated from the ventilation model. The total ventilation heat loss is

(A2) $$\Phi_v = \sum_{m=1}^{N} \Phi_v(m) = \dot{m}\, C_p [T_a(N) - T_a(0)]$$

The heat balance in the air node for each of the N-zones is obtained from the sum of the ventilation heat loss, $\Phi_v(m)$, the heat transferred by convection between the wall and the air, $\Phi_w(m)$, and the convective heat gain in zone m, $\Phi_g(m)$:

(A3) $$\Phi_v(m) + \Phi_w(m) + \Phi_g(m) = 0$$

The heat flow at the wall-air interface in zone m depends on the convective heat transfer coefficient and the heat exchanging surface area :

(A4) $$\Phi_w(m) = h_c\, S(m) [T_w(t,m) - T_a(m)]$$

The wall temperature in zone m depends on this heat flow :

(A5) $$T_w(m,t) = T_w(m,0) - \frac{2\Phi_w(m)}{S(m)\, b(m)} \sqrt{\frac{t}{\pi}}$$

Substitution of Eq. A5 into A4 gives :

$$\Phi_w(m) = h_c\, S(m) \left[T_w(m,0) - \frac{2\Phi_w(m)}{S(m)\, b(m)} \sqrt{\frac{t}{\pi}} - T_a(m) \right]$$

(A6) $$\Phi_w(m) = \left[h_c\, S(m)\, T_w(m,0) - \Phi_w(m) \frac{2h_c}{b(m)} \sqrt{\frac{t}{\pi}} - h_c\, S(m)\, T_a(m) \right]$$

and this is transformed into :

(A7) $$\Phi_w(m)\left[1+\frac{2h_c}{b(m)}\sqrt{\frac{t}{\pi}}\right] = h_c\,S(m)\,[\,T_w(m,0)-T_a(m)]$$

and using Eq. A1

(A8) $$\frac{\dot{m}\,C_p\,\delta T(m)}{h_c\,S(m)}\left[1+\frac{2h_c}{b(m)}\sqrt{\frac{t}{\pi}}\right] = T_w(m,0)-T_a(m-1)-\delta T(m)$$

Now the temperature of the mth zone, T(m), can be expressed into the temperature of the previous zone, T(m-1)

(A9) $$T_a(m) = T_a(m-1)+\frac{T_w(m,0)-T_a(m-1)}{\frac{\dot{m}\,C_p}{h_c\,S(m)}\left[1+\frac{2h_c}{b(m)}\sqrt{\frac{t}{\pi}}\right]+1}$$

Eq. A9, is a recurrence relation allowing to calculate $T_a(N)$, from the initial condition that $T_a(0)$ is the inlet air temperature (the outside temperature).

For fixed massflow (forced air flow) the calculation for each timestep is straightforward. However when the massflow depends on the inside temperature T_{in}, the latter is the unknown which is varied to obtain a solution by iteration until $T_{in} = T_a(N)$.

Once convergence is reached the zone air temperatures $T_a(m)$ are used to calculate the wall temperatures. From :

(A10) $$T_w(m,t)-T_w(m,0) = -\frac{2h_c}{b(m)}[T_w(m,t)-T_a(m)]\sqrt{\frac{t}{\pi}}$$

the wall temperature $T_w(m,t)$ is found :

(A11) $$T_w(m,t) = \frac{T_w(m,0)+T_a(m)\frac{2h_c}{b(m)}\sqrt{\frac{t}{\pi}}}{1+\frac{2h_c}{b(m)}\sqrt{\frac{t}{\pi}}}$$

and the heat transferred at the wall air interface in zone m, is calculated as

(A12) $$\Phi_w(m) = h_c\,S(m)\,[\,T_w(m,t)-T_a(m)]$$

The total ventilative heat flux is given by Eq. A2.

The way the wall thermal model takes the past thermal wall excitation into account is based on the assumption that the past is identical to the present. But in spite of this limitation the model shows the main features which are observed and can easily be improved.